Obscured AGN in a Strongly Lensed Giant Arc Revealed with Herschel

Michel Zamojski[1], Johan Richard[2] and the HLS Team

[1] Observatoire de l'Université de Genève, Switzerland

[2] Observatoire de Lyon, Université de Lyon 1, France

UNIVERSITÉ DE GENÈVE

FACULTÉ DES SCIENCES

Département d'astronomie

We present a detailed study of the infrared emission of the giant arc in the lensing cluster MACSJ0451+0006 with *Herschel*. This cluster was observed with both PACS and SPIRE as part of the *Herschel Lensing Survey* (HLS). The arc has a length of 20" and can, therefore, be decomposed in at least two components up to 250µm. We observe an excess of hot dust emission in the southern part of the arc, which we attribute to the presence of an obscured AGN. The arc is formed by the strong lensing (µ = 49) of a single source galaxy at $z = 2.014$ with a moderate instrinsic star formation rate (≈ 10 $M_\odot$ yr^{-1}) and stellar mass (≈ 5 × 10^9 $M_\odot$), making it representative of the bulk of the galaxy population at $z \approx 2$. The reconstructed morphology of the galaxy suggests an on-going merger. These results are in line with the common picture of AGN-galaxy co-evolution, but provide an example of such evolution taking place in a normal average galaxy at $z \approx 2$.

The giant arc in MACSJ0451+0006

The giant arc in the massive galaxy cluster MACSJ0451+0006 is created by the fortuitous alignment of the cluster and a galaxy at $z = 2.014$. Part of the galaxy crosses into a caustic region of the cluster in the source plane. The source is therefore strongly lensed: it has an average magnification factor of µ = 49. The part of the galaxy located inside the caustic is doubly-imaged and forms the northern part of the arc, whereas the southern part consists of a single stretched image of the rest of the galaxy. The arc was observed with, among others, the NIRSPEC spectrograph on the Keck **II** telescope (Richard et al. 2011), the OSIRIS IFU (Jones et al. 2010), and in CO with the plateau de Bure interferometer (Dessauges-Zavadsky et al. in preparation). The cluster has also been imaged with several telescopes including HST and *Chandra* (P.I. H. Ebeling) as well as with *Spitzer*/IRAC (channels 1 & 2 only) and *Herschel* (with both PACS and SPIRE) as part of the *IRAC* and *Herschel Lensing Surveys* (Egami et al. 2010). Figure 1 shows an RGB composite HST image of the arc, along with a source plane reconstruction in the F814W band. The source plane reconstruction is based on the mass model of Richard et al. (2011), and suggests an on-going merger. The integrated Hα flux of the galaxy translates into a star formation rate of ≈ 10 $M_\odot$ yr^{-1} (Jones et al. 2010) and a full UV-to-NIR SED analysis constrains its stellar mass to ≈ 5 × 10^9 $M_\odot$ (Sklias et al. 2013). These moderate properties make this galaxy an average and representative $z \approx 2$ main-sequence galaxy.

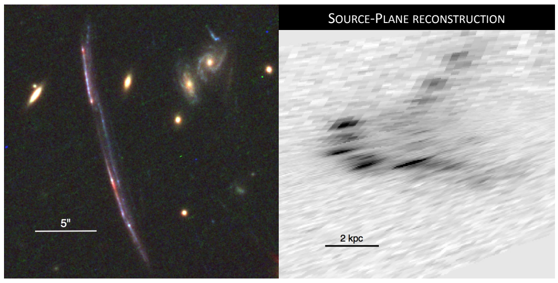

Figure 1: HST/F140W, F814W and F606W RGB composite image of the arc along with a source-plane reconstruction in F814W. The morphology suggests a merger.

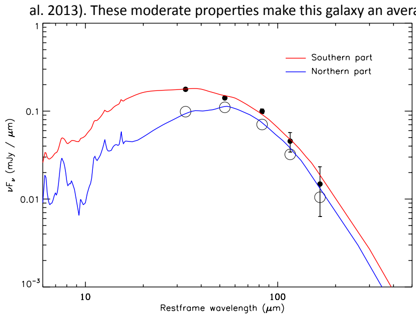

Figure 2: Best-fit SEDs of the northern and southern parts of the arc. The southern component shows an excess of hot dust emission at $\lambda_{rest} < 60$µm.

Infrared Photometry and SED

We have analyzed the multi-wavelength imaging dataset of the arc in a self-consistent manner. Part of these results are presented in Sklias et al. (2013), as well as in two companions posters by P. Sklias and D. Schaerer. Here, we focus on the IR emission as probed by *Herschel*. Figure 3 shows images of the arc overlaid in redscale consecutively with the PACS 100µm, 160µm, and the SPIRE 250, 350 and 500µm maps. From the PACS 100µm map, we observe a striking difference in the IR emission of the southern and northern parts of the arc, a difference that is not reproduced at other optical or IR wavelengths. We analyze the northern and southern components independently. In order to separate them, from each other as well as from surrounding sources, we use optical priors to fix the position of potential infrared bright sources and employ a PSF-fitting maximum likelihood algorithm to simultaneously solve for the flux of these sources (Guillaume et al. 2006, Zamojski 2008, Vibert et al. 2009). Starting at 100µm, we initially split the arc into three point sources: one for the south, and one for each of the northern images. We find the ratio of the fluxes of the two northern images to match the ratio of their magnification. We therefore fix this ratio when solving for the flux at 160µm and 250µm, effectively making it only two independent components. At 350µm and 500µm, the resolution becomes too coarse to allow us to even separate the northern and southern parts. At these wavelength we, therefore, simply fix the ratios of all parts of the arc to those measured at 250µm. The resulting SEDs of the northern and southern components are shown in Figure 2. They imply total intrinsic (i.e. after correcting for the magnification) IR-luminosities of 0.6 × 10^{11} $L_\odot$ in the north and 1.9 × 10^{11} $L_\odot$ in the south.

Figure 3

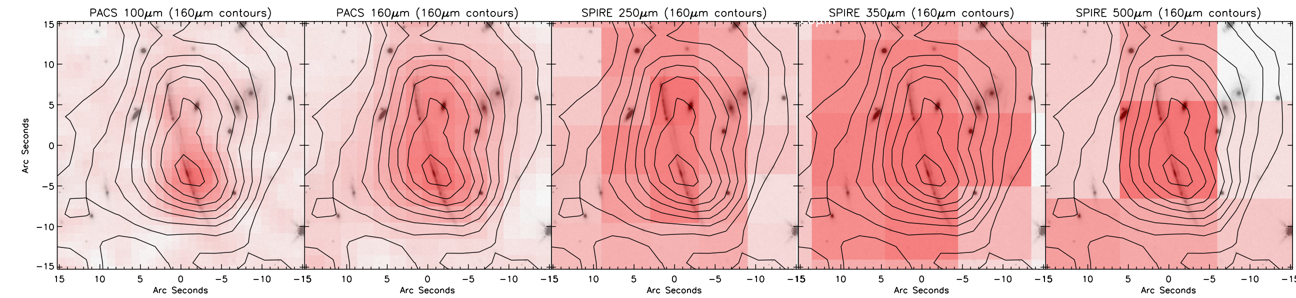

Evidence for an obscured AGN

Figure 2 shows the separate best-fit SEDs of the northern and southern parts of the arc. The SEDs are similar at long wavelengths but diverge shortward of 60µm restframe. The excess emission observed at 30µm restframe in the southern part of the arc cannot be reproduced with any starburst template. It requires an additional hot component, and is characteristic of the presence of an obscured AGN. We estimate the AGN contribution by decomposing the IR emission of the southern part of the arc into an AGN and a starburst component using the procedure of Mullaney et al. (2011), which combines an empirical AGN template with one of a series of starburst templates in proportions that best fit the observed SED. This is illustrated in Figure 4. Depending on the choice of starburst template, we find that the IR-luminosity of the southern component comes at only 30—50% from the host and is, therefore, dominated by the AGN. The inferred luminosity of the AGN is $L^{AGN}_{IR} \approx 1.0 \times 10^{11}$ $L_\odot$. When accounting for only the starburst component, the infrared flux of the arc is split between the northern and the southern parts in the same proportions as in the UV/optical.

Additional evidence for the presence of an AGN comes from the optical emission line ratios of the arc. Figure 5 shows that the arc lies in the AGN part of the BPT diagram, albeit in a scarcely population region of the plane. The arc is, however, not detected in *Chandra* down to a limiting flux of 1.25 × 10^{-14} erg cm^{-2} s^{-1}. This is one dex fainter than that expected from the average relation between $L_{0.5\text{-}10\ keV}$ and L^{AGN}_{IR} (Mullaney et al. 2011), and suggests a high level of obscuration.

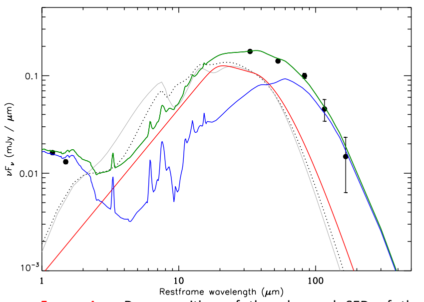

Figure 4: Decomposition of the observed SED of the southern part of the arc into its AGN (red) and starburst (blue) components using the empirical AGN template of Mullaney et al. (2011) and the starburst SED of M82. The sum of the two components is shown in green. Grey and dotted lines represents two clumpy torus models of Nenkova et al. (2008) for comparison. We require a steep mid-IR slope to match the IRAC photometry.

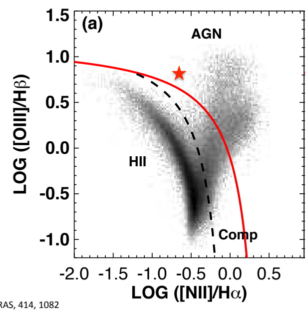

Figure 5: Position of the arc in the BPT diagram.

Summary

- From *Herschel* observations of the strongly lensed gravitational arc in MACS0451+0006, we have presented evidence for the presence of an obscured AGN in a moderate-mass average galaxy at $z \approx 2$.
- From a source-plane reconstruction of the galaxy, the presence of the obscured AGN appears to be concurrent with an on-going merger.

References

Egami, E., Rex M., Rawle T., et al. 2010, A&A, 518, L12
Guillaume, M., Llebaria, A., Aymeric, D., et al. 2006, SPIE, 6064, 332
Jones, T., Swinbank, A. M., Ellis R. S., et al. 2010, MNRAS, 404, 1247
Mullaney, J. R., Alexander, D. M., Goulding, A. D. & Hickox, R. C. 2011, MNRAS, 414, 1082
Nenkova, M., Sirocky, M. M, Nikutta, R., et al. 2008, ApJ, 685, 160
Richard, J., Jones, T., Ellis, R., et al. 2011, MNRAS, 413, 643
Sklias, P., Zamojski, M., Schaerer, D., et al. 2013, astro-ph/1310.2655
Vibert, D., Zamojski, M., Conseil, S., et al. 2009, SPIE, 7246, 23
Zamojski, Michel A. 2008, PhD Thesis, Columbia University